Nuclear Theory'21
ed. V. Nikolaev, Heron Press, Sofia, 2002

Nuclear Structure with the Dinuclear Model

G.G. Adamian[1], N.V. Antonenko[1], R.V. Jolos[1,2], Yu.V. Palchikov[1], W. Scheid[2] and T. Shneidman[2]

[1]Joint Institute for Nuclear Research, 141980 Dubna, Russia

[2]Institut für Theoretische Physik der Justus-Liebig-Universität, Giessen, Germany

Abstract.

The dinuclear system concept is applied to the explanation of the structure of nuclei. Hyperdeformed nuclei are assumed as dinuclear systems which could directly be excited in heavy ion collisions. Signatures of hyperdeformed states in such reactions could be γ-transitions between these states and their decay into the nuclei forming the hyperdeformed nucleus. The appearance of a low-lying band with negative parity states near the ground state band in actinide nuclei is explained by oscillations of the dinuclear system in the mass asymmetry coordinate. The results for the parity splitting and electric multipole moments in alternating parity bands in actinide nuclei are in agreement with experimental data.

1 Introduction

The dinuclear system (DNS) is a configuration with two touching nuclei which keep their individuality and exchange nucleons and/or clusters [1]. Such configurations are also denoted as quasimolecular or bi-cluster configurations and nuclear molecules [2]. Well known examples with light nuclei are the Be configuration built up by two touching α-particles and the nuclear molecular resonances in the reactions ^{12}C on ^{12}C up to ^{58}Ni on ^{58}Ni. The concept of the dinuclear system has manifold applications in the calculation of fusion cross sections for very heavy nuclei and of the mass and charge distributions in quasifission [3]. For example, in the production of superheavy elements, the DNS is first formed in the reaction between two heavy ions and then the touching nuclei exchange nucleons up to the moment when the system crosses the inner fusion barrier and an excited compound nucleus is formed.

In this review we discuss two applications of the DNS concept for the description of nuclear structure effects, First, in Section 2 we introduce the basic facts about the dinuclear system model. In Section 3 we study the question whether hyperdeformed states can be interpreted as dinuclear molecular resonances and propose the idea to produce hyperdeformed muclei in heavy ion reactions. Then, in Section 4 we explain the parity splitting of rotational bands in actinide nuclei where vibrations of the dinuclear system in the mass asymmetry coordinate about the shape of the compound nucleus are assumed.

2 Basic Facts on the Dinuclear Model

The main coordinates of the DNS model are the relative coordinate R between the nuclei (clusters) and the mass and charge asymmetry coordinates defined as $\eta = (A_1 - A_2)/(A_1 + A_2)$ and $\eta_Z = (Z_1 - Z_2)/(Z_1 + Z_2)$ where A_1, A_2 and Z_1, Z_2 are the mass and charge numbers of the nuclei, respectively. The potential of the DNS is strongly repulsive for smaller distances and hinders the nuclei to melt together in the relative coordinate. Under the assumption of a small overlap of the nuclei in the DNS, the potential energy is usually semi-phenomenologically calculated [4]

$$U(R, \eta, L) = B_1 + B_2 + V(R, \eta, L) - B_{12}. \tag{1}$$

Here, B_i ($i = 1, 2$, negative) are the asymptotic experimental binding energies of the nuclei, $V(R, \eta, L)$ is the interaction between the nuclei,

$$V(R, \eta, L) = V_C(R, \eta) + V_N(R, \eta) + V_{rot}(R, \eta, L), \tag{2}$$

consisting of the Coulomb potential, the nuclear part and the centrifugal potential $V_{rot} = \hbar^2 L(L+1)/(2\Im)$. The nuclear part is calculated by a double folding procedure with a Skyrme-type effective density-dependent nucleon-nucleon interaction taken from the theory of finite Fermi systems [5]. The potential $U(R, \eta, L)$ is related to the binding energy B_{12} of the compound nucleus. Also deformations of the clusters are taken into account by assuming the clusters in a pole-to-pole orientation.

The moment of inertia of the DNS can be assumed in the sticking limit

$$\Im = \Im_1 + \Im_2 + \mu R^2, \tag{3}$$

where μ is the reduced mass of relative motion and the moments of inertia $\Im_i$ ($i = 1, 2$) of the nuclei are calculated in the rigid body approximation.

Depending on the special application, the dynamics of the nuclear system on the potential energy surface can be treated by quantum mechanics in the case of low energies or statistically with the Fokker-Planck equation or master equations at higher excitation energies. In the case of nuclear structure effects we solve the corresponding Schrödinger equations in coordinates R and η.

3 Hyperdeformed Nuclei as Nuclear Molecules

Nuclear molecular states were first observed in the ^{12}C - ^{12}C collision by Bromley et al. [6] and then seen up to the system Ni + Ni by Cindro et al. [7]. The question arises whether heavier nuclear systems have excited states with the properties of molecular (or cluster) states. Such states could be the hyperdeformed (HD) states which are explained by nuclear shapes with a ratio of axes of $1:3$ caused by a third minimum in the potential energy surfaces (PES) of the corresponding nuclei. Very effective 4π γ-ray spectrometers like EUROBALL and GAMMASPHERE have been used in search for evidences for high-spin HD bands [8]. An interesting observation in shell model calculations was made that the third minimum of the PES of actinide nuclei belongs to a molecular configuration of two touching nuclei (clusters) which is a dinuclear configuration [9]. We showed that dinuclear systems have quadrupole moments and moments of inertia as those measured for superdeformed states and estimated for HD states [10].

If hyperdeformed states can be considered as quasimolecular resonance states, it should be possible to excite them by forming a hyperdeformed configuration in the scattering of heavy ions. In the following we discuss the systems ^{48}Ca + ^{140}Ce and ^{90}Zr + ^{90}Zr as possible candidates for exploring the properties of hyperdeformed states [11]. First, we calculated the potentials $V(R,\eta,L)$ with Eq. (2) as a function of the relative distance for various angular momenta. These potentials are shown in Figure 1. They have a minimum around 11 fm at a distance $R_m \approx R_1 + R_2 + 0.5$ fm where R_1 and R_2 are the radii of the nuclei. The depth of this molecular minimum decreases with growing angular momentum and vanishes for $L > 100$ in the considered systems.

The potential pocket has virtual and quasibound states situated above and below the barrier, respectively. Approximating the potential in the neighborhood of the minimum by a harmonic oscillator potential, we can easily estimate the positions of one to three quasibound states with an energy spacing of $\hbar\omega \approx 2.2$ MeV for $L > 40$. For example, in the ^{90}Zr + ^{90}Zr system we find the lowest quasibound state for $L = 50$ lying 1.1 MeV above the potential minimum.

The charge quadrupole moments of (40-50)$\cdot 10^2$ e fm^2 and the moments of inertia of (160-190) $\hbar^2$/MeV of the quasibound dinuclear configurations ^{48}Ca + ^{140}Ce and ^{90}Zr + ^{90}Zr are close to those estimated for hyperdeformed states. Therefore, we can assume that the quasibound states are HD states and propose to produce these states in heavy ion reactions of ^{48}Ca on ^{140}Ce and ^{90}Zr on ^{90}Zr. The following conditions should be fulfilled: 1. The quasibound states should be directly excited by tunneling through the potential barrier in R including the centrifugal potential, i.e. the DNS should have no extra excitation energy. 2. The DNS should stay in the potential minimum without changing the mass and charge asymmetries. Spherical and stiff nuclei (magic and double magic nuclei) fulfill the second condition.

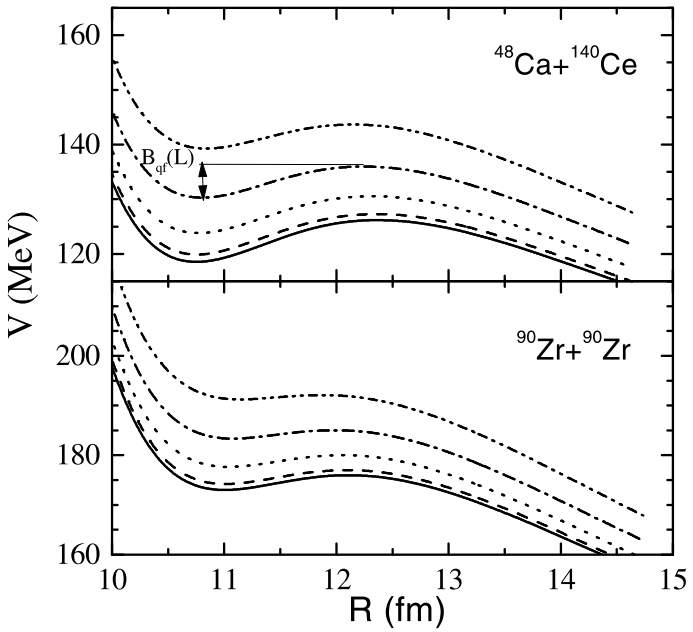

Figure 1. The potential $V(R, L)$ for the systems ^{48}Ca + ^{140}Ce (upper part) and ^{90}Zr + ^{90}Zr (lower part) as a function of R for $L = 0, 20, 40, 60, 80$ presented by solid, dashed, dotted, dashed-dotted and dashed-dotted-dotted curves, respectively.

The cross section for penetrating the barrier and populating quasibound states can be written as

$$\sigma(E_{c.m.}) = \frac{\pi\hbar^2}{2\mu E_{c.m.}} \sum_{L=L_{min}}^{L_{max}} (2L+1) T_L(E_{c.m.}). \tag{4}$$

Here, $E_{c.m.}$ is the incident energy in the center of mass system, $T_L(E_{c.m.})$ the transmission probability through the entrance barrier which is approximated by a parabola with frequency ω':

$$T_L(E_{c.m.}) = 1/\left(1 + \exp[2\pi(V(R_b, \eta, L) - E_{c.m.})/(\hbar\omega')]\right). \tag{5}$$

The barrier is at R_b. The angular momentum quantum numbers L_{min} and L_{max} in Eq. (4) fix the interval of angular momenta contributing to the excitation of HD states. The range of partial waves leading to the excitation of quasibound states constitutes the so called molecular window known in the theory of nuclear molecules with light heavy ions.

In the reaction ^{48}Ca on ^{140}Ce, cold and long living DNS states can be formed at an incident energy $E_{cm} = 147$ MeV and $90 < L < 100$, and in the reaction

^{90}Zr on ^{90}Zr at $E_{c.m} = 180$ MeV and $40 < L < 50$. For both reactions we estimate a cross section (4) of about 1 μb. Also other reactions, namely ^{48}Ca + ^{144}Sm ($E_{c.m} = 149$ MeV, $80 < L < 90$), ^{48}Ca + ^{142}Nd ($E_{c.m} = 148$ MeV, $80 < L < 90$), and ^{38}Ar + ^{140}Ce, ^{142}Nd, ^{144}Sm ($E_{c.m} = 137, 141$ and 145 MeV, respectively, $80 < L < 90$) can be thought to be applied for a possible observation of cluster-type HD states.

The spectroscopic investigation of the HD structures is difficult because of the small formation cross section and the high background produced by fusion-fission, quasifission and other reactions. However, the later processes have characteristic times much shorter than the life-time of the HD states which is of the order of 10^{-16} s. Therefore, the HD states should show up as sharp resonance lines as a function of the incident energy.

4 Cluster Interpretation of Alternating Parity Bands in Actinides

The appearance of a low-lying band with negative parity states near the positive parity ground state band of even-even actinide nuclei as Ra, Th, U and Pu is caused by reflection asymmetric shapes of these nuclei [12, 13]. The negative parity states are shifted upwards with respect to the positive parity states. This effect is denoted as parity splitting. The band with negative parity and the parity splitting can be explained by considering the dynamics in the octupole deformation degree of freedom [14,15] or by assuming vibrations in the mass asymmetry degree of freedom [16]. The later type of approach is based on a cluster interpretation of low-lying negative parity states and can be formulated in the dinuclear model. This approach will be used in the following to explain the parity splitting and to calculate electric dipole, quadrupole and octupole transition moments observed in alternating parity bands in actinide nuclei.

Instead of a parametrization of the nuclear shape in terms of quadrupole, octupole and higher multipole deformations, we use the mass asymmetry coordinate η as the relevant collective variable. The ground state wave function in η is thought as a superposition of different cluster-type configurations including the mono-nucleus configuration $|\eta| = 1$. Calculating the potential energy of the dinuclear system for the actinide nuclei, we find an alpha-cluster configuration mixed to the ground state wave function :

$$^{A}Z \rightarrow ^{(A-4)} (Z-2) + \alpha \text{ - particle.}$$

The mono-nucleus configuration has a higher energy than the alpha-cluster configuration. The resulting potential is schematically depicted as a function of the mass asymmetry coordinate in Figure 2, where also the reflection-asymmetric shapes of the alpha-cluster configuration are shown. The mass asymmetry coordinates of the later configurations are $\eta_\alpha = \pm(1 - 8/A)$.

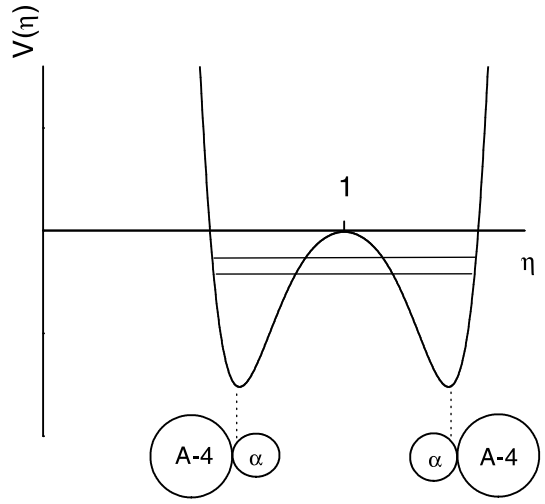

Figure 2. Schematic picture of the potential in the mass asymmetry and of the two states with different parities (parallel lines, lower state with positive parity, higher state with negative parity).

Since the potential energy of configurations with a light cluster heavier than an alpha-particle increases rapidly with decreasing $|\eta|$, we restricted our investigations to configurations with light clusters not heavier than Li, i.e. to cluster configurations near $|\eta| = 1$, and not too high angular momenta.

It is convenient to substitute the coordinate η by the following coordinate

$$x = \eta - 1 \text{ if } \eta > 0,$$
$$x = \eta + 1 \text{ if } \eta < 0.$$

Then the Schrödinger equation can be written as

$$\left(-\frac{\hbar^2}{2B_x}\frac{d^2}{dx^2} + U(x,I)\right)\psi_n(x,I) = E_n(I)\psi_n(x,I), \tag{6}$$

where $B_x = B_\eta$ is the effective mass. The potential energy is calculated with Eq. (1) by setting $U(x,I) = U(R = R_m, \eta, L = I)$ with the touching distance R_m between the clusters. Details of the calculation of $V_N(R_m,\eta)$ are given in [4]. The nuclear density distribution is approximated by the Fermi distribution with a radius parameter of 1.15 fm for the Ra - Pu region and with a diffuseness parameter $a = 0.48$ fm for the densities of ^{4}He and ^{7}Li and $a = 0.56$ fm $(B_n^{(0)}/B_n)^{1/2}$ for the heavy clusters, where B_n and $B_n^{(0)}$ are the neutron binding energies of the

studied nucleus and of the heaviest isotope considered for the same element, respectively. For example in the case of Ra, Th and U isotopes, $B_n^{(0)}$ corresponds to the neutron binding energies of ^{226}Ra, ^{232}Th and^{238}U, respectively. To calculate the potential energy for $I \neq 0$, the moment of inertia $\Im$ in the centrifugal potential is expressed for cluster configurations with α and Li as light clusters as

$$\Im(\eta) = c_1(\Im_1^r + \Im_2^r + M\frac{A_1A_2}{A}R_m^2). \tag{7}$$

Here, $\Im_i^r$ ($i = 1, 2$) are the rigid body moments of inertia for the clusters of the DNS, $c_1 = 0.85$ for all considered nuclei and M is the nucleon mass. Single particle effects like alignment of the single particle angular momenta in the heavy cluster are neglected.

For $|\eta| = 1$, the moment of inertia is not known from the data because the experimental moment of inertia is a mean value between the moments of inertia of the mono-nucleus ($|\eta| = 1$) and of the cluster configurations arising due to oscillations in η. We assume

$$\Im(|\eta| = 1) = c_2\Im^r(|\eta| = 1). \tag{8}$$

Here, $\Im^r$ is the rigid body moment of inertia of the mono-nucleus calculated with deformation parameters and $c_2 = 0.1 - 0.3$ a scaling parameter fixed by the energy of the first 2^+ state. For example, for the isotopes ^{220,222,224,226}Ra we find $\Im(|\eta = 1) = 12, 17, 22,$ and $32\hbar^2/$MeV, respectively.

Then a smooth parametrization of the potential $U(x, I)$ is chosen:

$$U(x, I) = \sum_{k=0}^{4} a_{2k}(I)x^{2k}. \tag{9}$$

The parameters $a_{2k}(I)$ with $k > 0$ are determined by the calculated potential values for $x = x_\alpha$ and $x = x_{Li}$. The value $a_0(I = 0)$ is taken so that the ground state energy $E_0(I = 0)$ is zero after the solution of the Schrödinger equation. In the majority of cases this procedure leads to a value $U(x = 0, I = 0) = a_0(I = 0)$ close to $E_0(I = 0) = 0$. However, for ^{222}Th and ^{220,222}Ra we varied the inertia coefficient $B_x = B_\eta$ in Eq. (6) in the range $B_\eta = (10 - 20) \times 10^4 M$ fm^2 to obtain the correct value of $E_0(I = 0) = 0$. In the other cases we set $B_\eta = 20 \times 10^4 M$ fm^2 with a variation of 10%.

The mass B_η can be estimated by relating the mass asymmetry coordinate η to the octupole deformation coordinate β_3. Such a relation between η, R and β_3 was derived in [10]:

$$\beta_3 = \sqrt{\frac{7}{4\pi}}\frac{\pi}{3}\eta(1 - \eta^2)\frac{R^3}{R_0^3}, \tag{10}$$

where R_0 is the spherical equivalent radius of the corresponding compound nucleus. If we take the value of $B_{\beta_3} = 200\hbar^2 MeV^{-1}$ known from the literature [17], then we obtain $B_\eta \approx (d\beta_3/d\eta)^2 B_{\beta_3} = 9.3 \times 10^4 M$ fm^2, compatible with the one used in the calculations.

We first calculated the parity splitting for several isotopes of Ra, Th, U and Pu for different values of the nuclear spin I. Figure 3 gives a comparison of experimental and calculated energies of states of the alternating parity bands in $^{232-238}$U. The experimental data are taken from [18,19]. Also the results for the other isotopes agree well with the experimental data with the largest deviations in the lightest Ra and Th isotopes.

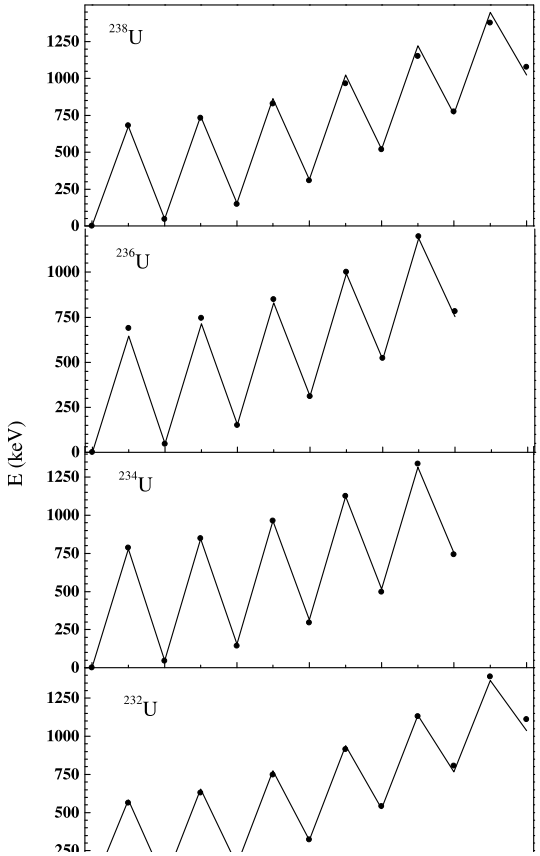

Figure 3. Experimental (points) and theoretical (lines) rotational spectra for ^{238,236,234,232}U.

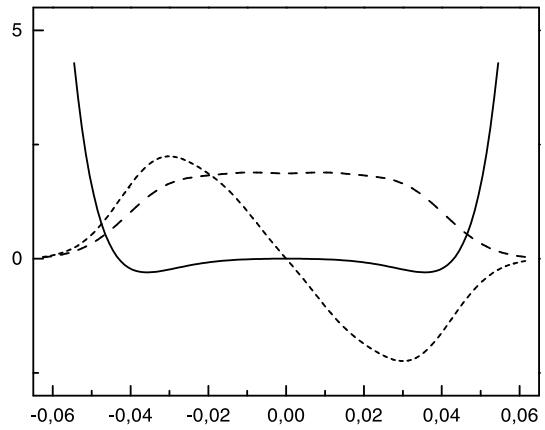

Figure 4. Potential energy (solid curve) and wave functions of 0^+ (long-dashed curve) and 1^- (short-dashed curve) states of ^{224}Ra.

The ground state wave function has a maximum in the vicinity of $|\eta| = 1$ even when the potential energy has minima at $|\eta| = \eta_\alpha$ because these minima of maximal 0.8 MeV are rather shallow as shown in Figure 4. With increasing angular momentum the barrier at $x = 0$ separating the minima at $|x| = x_\alpha$ increases and the maxima of the wave function shift closer to the minima of the potential, i.e. to the α-cluster configuration. In the ground state of ^{226}Ra we find a weight of the α-cluster configuration, estimated as that contribution to the norm of the wave function located at $|x| \geq x_\alpha$, of about 5×10^{-2} which is close to the calculated spectroscopic factor [20].

A good test for the quality of the calculations are the reduced matrix elements of the electric multipole moments $Q(E1), Q(E2)$ and $Q(E3)$. The electric multipole operators can be obtained for the dinuclear system and result in the expressions [10]:

$$Q_{10} = 2D_{10} = e\frac{A}{2}(1-\eta^2)R_m(\frac{Z_1}{A_1} - \frac{Z_2}{A_2}), \tag{11}$$

$$Q_{20} = e\frac{A}{4}(1-\eta^2)R_m^2((1-\eta)\frac{Z_1}{A_1} + (1+\eta)\frac{Z_2}{A_2}) + Q_{20}(1) + Q_{20}(2), \tag{12}$$

$$Q_{30} = e\frac{A}{8}(1-\eta^2)R_m^3((1-\eta)\frac{Z_1}{A_1} - (1+\eta)\frac{Z_2}{A_2}) + \frac{3}{2}((1-\eta)^2 Q_{20}(1) - (1+\eta)^2 Q_{20}(2)), \tag{13}$$

where the charge quadrupole moments $Q_{20}(i)$ of the clusters $i = 1, 2$ are calculated with respect to their centers of mass. The charge-to-mass ratios Z_1/A_1

and Z_2/A_2 are functions of η. For the α-particle this ratio is equal to 0.5. For small values of $|x|$ we parametrize the ratio Z/A of the light cluster as following: Z/A is equal to the value of the mono-nucleus for $|x| < x_\alpha$ and $Z/A = 0.5$ for $|x| \geq x_\alpha$ as for the α-cluster.

In Eqs. (11)–(12) we use effective charges e^{eff} instead of the unit charge e. We set the effective charge for $E1$-transitions to be $e_1^{eff} = e(1 + \chi)$ with an average state-independent value of the $E1$ polarizability coefficient $\chi = -0.7$. This renormalization regards a coupling of the mass-asymmetry mode to the giant dipole resonance. For quadrupole transitions we set $e_2^{eff} = e$ although an effective charge of $1.35e$ describes the experimental data better. Octupole transitions are treated with $e_{3,proton}^{eff} = 1.2e$ and $e_{3,neutron}^{eff} = 0.8e$ by assuming effects from the coupling of the mass-asymmetry mode with higher-lying isovector and isoscalar octupole excitations.

Figures 5 - 7 show calculated reduced electric multipole moments for ^{226}Ra as a function of nuclear spin in comparison with experimental data (from [21]). The obtained values (also of other actinides) are in qualitative agreement with the known experimental data for Q_λ^{exp} with some exceptions, e.g. in the case of ^{220,222}Ra.

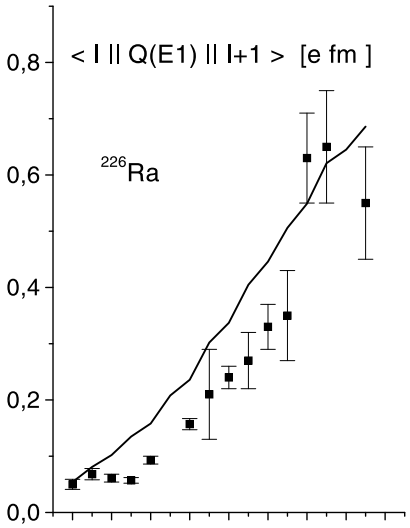

Figure 5. Reduced matrix elements of the electric dipole operator (solid curve) for ^{226}Ra in comparison with experimental data (squares).

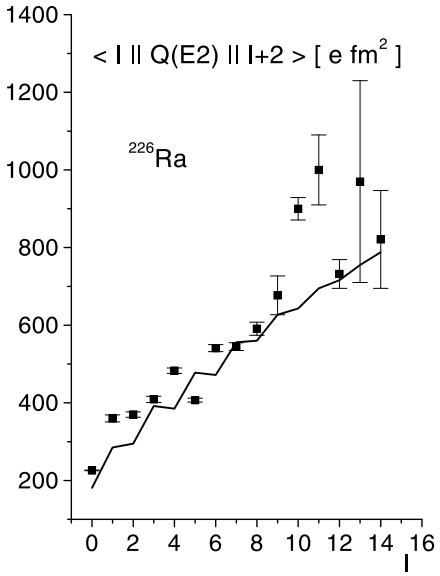

Figure 6. The same as in Figure 5 , but for the quadrupole operator.

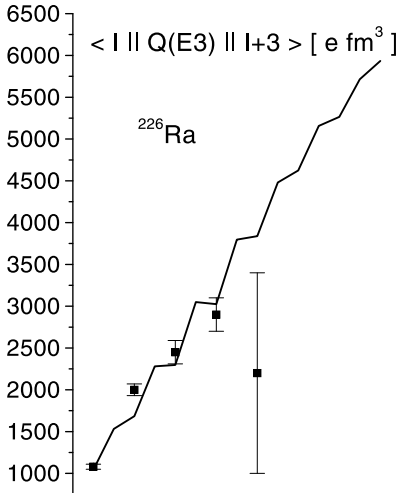

Figure 7. The same as in Figure 5 , but for the octupole operator.

5 Summary

Nuclear structure phenomena can be explained by selected states of the dinuclear system. We distinguish two types of states: states in the relative motion of the clusters and states in the mass asymmetry degree of freedom. The first type of states is used to interpret states of hyperdeformed nuclei as quasimolecular resonances in the nucleus-nucleus potential of heavy nuclei. These states are characterized by γ-transitions between HD states and by their decay into the nuclei by which they are formed. Therefore, if these signatures would be observed in heavy ion experiments, it would be an unique proof of the idea that HD states are cluster-type states and further that quasimolecular configurations also exist in heavier nuclear systems.

The cluster interpretation of the properties of the alternating parity bands of Ra, Th, U and Pu isotopes is based on collective states in the mass asymmetry degree of freedom. The calculated parity splitting and the multipole transition moments reproduce the experimental data quite well. This agreement gives a strong impulse for research on the appearance of further possible long living states in the mass asymmetry degree of freedom which would complement the statistical behaviour of this degree of freedom at higher energies studied in fusion and quasifission reactions.

References

[1] V.V. Volkov, (1986) *Izv. AN SSSR ser. fiz.* **50** 1879; V.V. Volkov, (1982) *Deep Inelastic Nuclear Reactions* (Energoizdat, Moscow).

[2] W. Greiner, J.Y. Park and W. Scheid, (1995) *Nuclear Molecules* (World Scientific, Singapore).

[3] G.G. Adamian, N.V. Antonenko, E.A. Cherepanov, S.P. Ivanova, R.V. Jolos, A.K. Nasirov, V.V. Volkov, A. Diaz Torres, W. Scheid and T.M. Shneidman, (2002) *Dinuclear System Model for Dynamics and Nuclear Structure* in: Proceedings of the Conf. on Exotic Nuclei, Baikal Lake, 2001, (eds. by Yu. Oganessian *et al.*; World Scientific, Singapore).

[4] G.G. Adamian, N.V. Antonenko, R.V. Jolos, S.P. Ivanova and O.I. Melnikova, (1996) *Int. J. Mod. Phys.* **E5** 191.

[5] A.B. Migdal, (1982) *Theory of Finite Fermi Systems and Application to Atomic Nuclei* (Nauka, Moscow).

[6] D.A. Bromley, J.A. Kuehner and E. Almqvist, (1960) *Phys. Rev. Lett.* **4** 365.

[7] L. Vannucci, N. Cindro *et al.*, (1996) *Z. Phys.* **A355** 41.

[8] A. Krasznahorkay *et al.*, (1999) *Phys. Lett.* **B461** 15; (1998) *Phys. Rev. Lett.* **80** 2073.

[9] S. Cwiok, W. Nazarewicz, J.X. Saladin, W. Plociennik and A. Johnson, (1994) *Phys. Lett.* **B322** 304.

[10] T.M. Shneidman, G.G. Adamian, N.V. Antonenko, S.P. Ivanova and W. Scheid, (2000) *Nucl. Phys.* **A671** 119.

[11] G.G. Adamian, N.V. Antonenko, N. Nenoff and W. Scheid, (2001) *Pys. Rev.* **C64** 014306.

[12] I. Ahmad and P.A. Butler, (1993) *Ann. Rev. Nucl. Part. Sci.* **43** 71.

[13] P.A. Butler and W. Nazarewicz, (1996) *Rev. Mod. Phys.* **68** 350.

[14] J.L. Egido and L.M. Robledo, (1990) *Nucl. Phys.* **A518** 475.

[15] E. Garrote, J.L. Egido, and L.M. Robledo, (1998) *Phys. Rev. Lett.* **80** 4398.

[16] T.M. Shneidman, G.G. Adamian, N.V. Antonenko, R.V. Jolos, W. Scheid, (2002) *Phys. Lett.* **B526** 322.

[17] G.A. Leander, R.K. Sheline, P. Möller, P. Olanders, I. Ragnarsson, A.J. Sirk, (1982) *Nucl. Phys.* **A388** 452.

[18] *http://www.nndc.bnl.gov/nndc/ensdf/*.

[19] J.F.C. Cocks *et al.*, (1999) *Nucl. Phys.* **A645** 61.

[20] Yu.S. Zamiatin *et al.*, (1990) *Phys. Part. Nucl.* **21** 537.

[21] H.J. Wollersheim *et al.*, (1993) *Nucl. Phys.* **A556** 261.